

The Pennsylvania State University
The Graduate School
College of Earth and Mineral Sciences

**MECHANISMS OF SINTERING AND SECOND PHASE
FORMATION IN BAYER ALUMINA**

A Dissertation in
Materials Science and Engineering
by
Tobias Frueh

© 2017 Tobias Frueh

Submitted in Partial Fulfillment
of the Requirements
for the Degree of

Doctor of Philosophy

September 2017

The dissertation of Tobias Frueh was reviewed and approved* by the following:

Gary Messing

Distinguished Professor of Ceramic Science and Engineering

Thesis Advisor, Chair of Committee

James Adair

Professor of Materials Science and Engineering, Biomedical Engineering and
Pharmacology

Optional Title Here

John Hellmann

Professor of Materials Science and Engineering

Associate Dean for Graduate Education and Research

Dogulas Wolfe

Associate Professor of Materials Science and Engineering

Department Head, Advanced Coatings at the Applied Research Laboratory

Senior Scientist

*Signatures are on file in the Graduate School.

Abstract

Table of Contents

List of Figures	vi
List of Tables	vii
Acknowledgments	viii
Chapter 1	
Statement of Problem	2
1.1 section1.1	2
1.1.1 subsection1.1.1	2
Chapter 2	
Introduction	3
2.1 section2.1	3
2.2 section2.2	3
Chapter 3	
The Effects of Na₂O and SiO₂ on Liquid Phase Sintering of Bayer Al₂O₃	4
3.1 Introduction	4
3.2 Experimental	5
3.3 Results	6
3.3.1 Effects of Na ₂ O-doping	6
3.3.2 Effects of Na ₂ O/SiO ₂ co-doping	7
3.4 Discussion	8
3.5 Summary	13
Chapter 4	
Powder Chemistry Effects on the Sintering Behavior of MgO-doped Bayer Alumina	26

4.1	Introduction	26
4.2	More Declaration	26
4.2.1	Some nonsense here	27
4.2.2	Some additional nonsense here	27
Chapter 5		
	Powder Chemistry Effects on Grain Boundaries During Densi- fication of Bayer Alumina	28
5.1	Introduction	28
5.2	More Declaration	28
Chapter 6		
	β-Al₂O₃: A Model System for the Formation of Second Phases in Al₂O₃	30
6.1	Introduction	30
6.2	More Declaration	30
Chapter 7		
	Summary and Future Work	32
7.1	Introduction	32
7.2	More Declaration	32
	Bibliography	34

List of Figures

3.1	SEM image of as-received chemically purified Bayer Al_2O_3 powder used in this study.	17
3.2	Dilatometer curves of as-received and singly Na_2O -doped samples heated at $10^\circ\text{C}/\text{min}$ to 1525°C	18
3.3	Densification kinetics of Bayer Al_2O_3 doped with different Na_2O concentrations and sintered at 1525°C	19
3.4	Microstructures of as-received and singly 529 ppm Na_2O doped samples after 30 min, 3 h and 8 h at 1525°C	20
3.5	Dilatometer curves of as-received, singly SiO_2 -doped, and $\text{Na}_2\text{O}/\text{SiO}_2$ -doped Bayer Al_2O_3 heated at $10^\circ\text{C}/\text{min}$ to 1525°C	21
3.6	Densification kinetics of Bayer Al_2O_3 doped with different concentrations of Na_2O and SiO_2 at 1525°C	22
3.7	Microstructures of Bayer Al_2O_3 doped with a) 603 ppm SiO_2 and b) 529 ppm Na_2O and 603 ppm SiO_2 after heating at 1525°C for 8h.	23
3.8	Micrographs of a sample doped with 1029 ppm Na_2O after sintering at 1525°C for 3 h. The micrographs were recorded using a) a secondary electron detector and b) a backscattered electron detector. The arrows point at the platelet shaped beta alumina grains that form in samples doped with Na_2O . The samples were not thermally etched.	24
3.9	Liquidus projection of the Al_2O_3 - SiO_2 - Na_2O ternary phase diagram. The red solid lines are isoplethal cuts representing the samples investigated in this study. The red dashed line is the 1525°C isotherm where α - Al_2O_3 and liquid are in equilibrium. The blue dash-dot line and green dotted line are eutectic lines at which α - Al_2O_3 and liquid is in equilibrium with β - Al_2O_3 or mullite, respectively.	25

List of Tables

3.1	Physical and chemical characteristics of the as-received Bayer Al_2O_3 powder used in this study.	15
3.2	Calculated compositions and amounts of liquid in as-received, singly doped and co-doped samples at 1525°C ($\alpha = \alpha\text{-Al}_2\text{O}_3$, $\beta = \beta\text{-Al}_2\text{O}_3$, L = liquid, M = mullite).	16

Acknowledgments

Dedication

Chapter 1 |

Statement of Problem

1.1 section1.1

Pestorius [200] developed an algorithm to investigate propagation of finite-amplitude noise in pipes. His algorithm, based on weak shock theory, includes the effects of nonlinearity and tube wall boundary layer attenuation and dispersion. The hybrid time-frequency domain algorithm applies nonlinearity in the time domain, applies a fast Fourier transform (FFT), and then applies attenuation and dispersion in the frequency domain. Then an inverse FFT is taken to return to the time domain to propagate to the next step.

1.1.1 subsection1.1.1

Chapter 2 | Introduction

2.1 section2.1

When in the Course of human events, it becomes necessary for one people to dissolve the political bands which have connected them with another, and to assume among the powers of the earth, the separate and equal station to which the Laws of Nature and of Nature's God entitle them, a decent respect to the opinions of mankind requires that they should declare the causes which impel them to the separation.

2.2 section2.2

Chapter 3 |

The Effects of Na_2O and SiO_2 on Liquid Phase Sintering of Bayer Al_2O_3

3.1 Introduction

Al_2O_3 is arguably the most extensively used and researched ceramic material because it is used in many large volume applications such as high temperature refractories, technical ceramics, high voltage insulators, and functional fillers. The majority of Al_2O_3 applications use synthetic or specialty aluminas derived from Bayer feedstocks, such as aluminum trihydrate ($\text{Al}(\text{OH})_3$), smelter grade Al_2O_3 and others. Bayer process aluminas are typically 99.0 - 99.9% pure and contain Na_2O , CaO , Fe_2O_3 , and SiO_2 impurities that originate from the bauxite ore and/or Bayer process reagents (e.g., NaOH). The vast majority of research on the sintering of Al_2O_3 , however, focuses on ultra-high purity ($\geq 99.99\%$) aluminas derived from specialty feedstocks, such as ammonium alum ($\text{NH}_4\text{Al}(\text{SO}_4)_2 \cdot 12\text{H}_2\text{O}$), boehmite ($\gamma\text{-AlOOH}$) and aluminum chloride (AlCl_3). While ultra-high purity aluminas provide the purest platform from which to conduct fundamental sintering research, that research does not usually explore the types and amounts of impurities typical of Bayer aluminas. Commercial Bayer Al_2O_3 powders exist in a range of reactive grades that differ in the amount and types of these impurities. Therefore, the evaluation of specialty reactive aluminas, within the context of previous work on ultra-high purity aluminas, is a valuable contribution to industrial users and bridges

fundamental sintering research with ultra-high purity aluminas.

3.2 Experimental

A chemically purified 0.4 μm median particle size Bayer process Al_2O_3 powder (Almatis, Inc., Leetsdale, PA, USA) with only 2 ppm MgO was used to study the sintering of near MgO-free Bayer Al_2O_3 (Figure 3.1). The powder was chemically purified by the manufacturer so that impurity levels similar to commercial high purity Bayer process aluminas were obtained after doping with Na_2O and/or SiO_2 . The physical and chemical characteristics of the as-received powder are shown in Table 3.1. Chemical analysis of the as-received Al_2O_3 was performed by inductively coupled plasma (ICP) emission spectroscopy (iCap 6000, Thermo Fischer Scientific, Inc., Waltham, MA, USA) after Al_2O_3 samples were acid digested in a microwave digestion unit in a TeflonTM sample holder. It should be noted that the as-received Bayer Al_2O_3 contained impurity levels of 90 ppm Fe_2O_3 , 62 CaO, and 22 ppm TiO_2 . The Na_2O and SiO_2 reported after doping include the impurity concentrations in the as-received powder (29 ppm Na_2O and 103 ppm SiO_2).

The Al_2O_3 powders were doped with up to 1000 ppm Na_2O using sodium acetate ($\text{NaC}_2\text{H}_3\text{O}_2 \cdot 3\text{H}_2\text{O}$, ACS grade, BDH, West Chester, PA, USA), based on the procedure reported by Louet et al. [1]. The Al_2O_3 powders were dispersed in a solution of sodium acetate dissolved in de-ionized water. The suspension was stirred on a magnetic stir plate for 5 h at room temperature, and held at 80°C for 24 h while stirring until the mixture was too viscous to stir, and then dried at 100°C for 24 h.

Samples were doped with up to 500 ppm SiO_2 by first dissolving tetraethyl orthosilicate (TEOS, $\text{Si}(\text{OC}_2\text{H}_5)_4$, 98%, Aldrich Chemical Company, Inc., Milwaukee, WI, USA) in 200 proof ethanol with a few drops of de-ionized water to hydrolyze the TEOS and immediately mixed at room temperature for 5 h with either the as-received or Na_2O -doped Al_2O_3 powder. The mixture was subsequently stirred at 70°C for an additional 12 h. The powder was then dried at 100°C for 2 h, followed by crushing in a mortar and pestle, and sieving to $-106 \mu\text{m}$ (US Standard 140 mesh).

Samples were prepared for sintering studies by uniaxially dry pressing the powders at 170 MPa and then cold isostatic pressing at 200 MPa (CIP, Autoclave

Engineers, Erie, PA, USA) to obtain cylindrical samples (3.0-3.5 mm long by 12.7 mm diameter or 8.5-10 mm long by 6 mm diameter) with green densities of $59.0\% \pm 0.5\%$ of theoretical density. To investigate the sintering process, dry pressed 8.5-10 mm long by 6 mm diameter cylinders were heated at $10^{\circ}\text{C}/\text{min}$ to 1525°C in a thermomechanical analyzer (TMA, Linseis PT1600, Robbinsville, NJ, USA). The kinetics of sintering and grain growth were evaluated on 3.0-3.5 mm long by 12.7 mm diameter samples heated at $10^{\circ}\text{C}/\text{min}$ to 1200°C then $5^{\circ}\text{C}/\text{min}$ to 1525°C followed by sintering at 1525°C for up to 8 h. The density of three samples of each condition was measured by the Archimedes method according to ASTM standard B962-15 [2] and the average density reported for each sintering time and temperature. For microstructure analysis, samples were first polished to a surface finish of $1\ \mu\text{m}$ and then thermally etched in air at 1425°C for 40 min. Average grain sizes were measured on SEM (ESEM, Quanta 200, FEI Company, Hillsboro, OR, USA) micrographs using a linear intercept method (ASTM Standard E112-96) [3].

3.3 Results

3.3.1 Effects of Na_2O -doping

The doping experiments were designed to uniformly distribute Na_2O and SiO_2 on the surfaces of the Al_2O_3 particles. Upon heating the dopant $\text{NaC}_2\text{H}_3\text{O}_2 \cdot 3\text{H}_2\text{O}$ first dehydrates and then decomposes to form Na_2CO_3 above 385°C [4]. Using a video recorder, we observed that anhydrous sodium acetate melts and rapidly spreads on the surface of an Al_2O_3 substrate at $\sim 420^{\circ}\text{C}$. Na_2CO_3 melts at 851°C and subsequently decomposes to Na_2O [4]. As a result of the rapid wetting of the Na_2O precursor on the Al_2O_3 substrate we conclude that Na_2O is uniformly distributed on the powder surface by the acetate doping process.

Figure 3.2 shows the shrinkage behavior of Bayer Al_2O_3 doped with different Na_2O concentrations during heating to 1525°C at $10^{\circ}\text{C}/\text{min}$. The as-received Al_2O_3 (intrinsic impurities: 29 ppm Na_2O , 103 ppm SiO_2) begins to shrink at $\sim 1050^{\circ}\text{C}$, whereas shrinkage begins at 1100°C for samples doped with 1029 ppm Na_2O . The difference in density at the beginning of densification continues throughout the heating cycle. However, above $\sim 1350^{\circ}\text{C}$ the densification rate of the Na_2O doped samples surpasses that of the as-received sample. Overall, the Na_2O -doped samples

are 2.5% less dense than the as-received Al_2O_3 after heating to 1525°C .

Figure 3.3 shows the influence of Na_2O concentration on the densification kinetics at 1525°C . Clearly, the degree of densification decreases with increasing Na_2O concentration for up to 30 min with the Na_2O -doped samples being as much as 2% less dense than the as-received Al_2O_3 . However, after ≥ 30 min at 1525°C densification is independent of Na_2O content and all samples are 97.5-98.0% dense after ≥ 3 h.

The microstructures of as-received samples (29 ppm Na_2O) and samples doped with 529 ppm Na_2O sintered for 30 min, 3 h and 8 h at 1525°C are compared in Figure 3.4. It is seen that higher Na_2O concentration does not affect the average grain size for all hold times. Microstructures of as-received samples are predominantly equiaxed with a small number of faceted grains, whereas samples doped with Na_2O appear to have an increasing number of faceted grain boundaries with increasing Na_2O concentration. A few tabular grains of up to $60\text{ }\mu\text{m}$ were seen in both as-received and Na_2O -doped samples after 8 h at 1525°C (see Figure 3.4c and 3.4f). Those faceted grains are larger in the as-received powder samples compared to Na_2O -doped samples, whereas the Na_2O -doped samples show more large tabular grains than samples from the as-received powder.

3.3.2 Effects of $\text{Na}_2\text{O}/\text{SiO}_2$ co-doping

As seen in Figure 3.5, the presence of 603 ppm SiO_2 significantly retards densification of as-received alumina. Starting at $\sim 1250^\circ\text{C}$, all of the SiO_2 -doped samples densify less than as-received and singly Na_2O -doped samples. The densification rate of the SiO_2 -doped samples from 1250 to 1525°C is slower than the as-received alumina. SiO_2 reduces the linear shrinkage by $\sim 3.0\%$ and thus the samples are 8.7% less dense than the as-received Al_2O_3 after 8 h at 1525°C .

The densification kinetics of the Al_2O_3 powders doped with different amounts of Na_2O (154 and 529 ppm) and SiO_2 (203 and 603 ppm) are compared in Figure 3.6. It is seen that the addition of SiO_2 significantly reduces sintered density for all hold times. For example, samples containing as much as 603 ppm SiO_2 have densities of 81.5% after 0 h and 93.8% after 8 h at 1525°C , whereas the as-received and singly Na_2O -doped Al_2O_3 samples are 98% dense after 3 h at 1525°C .

Figure 3.6 shows the effect of Na_2O on the densification of SiO_2 -doped samples.

For hold times < 1 h, samples doped with 529 ppm Na₂O and 203 ppm SiO₂ are $\sim 1.5\%$ denser than samples doped with 154 ppm Na₂O and 203 ppm SiO₂. A difference in Na₂O concentration does not affect the final density of samples containing 203 ppm SiO₂ (96.5 - 97.0%) after 3 h at 1525°C. For higher SiO₂ concentrations (603 ppm), singly SiO₂ doped samples are 1 - 2.5% less dense than samples co-doped with 529 ppm Na₂O and 603 ppm SiO₂ for all hold times at 1525°C.

The average grain sizes of the as-received and Na₂O-doped samples are nominally the same and increase from 1.6 μm to 2.5 μm after 30 min and 8 h at 1525°C, respectively. There was little grain growth (1.4 μm to 2.1 μm) in singly SiO₂-doped samples (603 ppm) after 30 min and 8 h at 1525°C, respectively. In samples co-doped with 529 ppm Na₂O and 603 ppm SiO₂ the average grain size is 1.6 μm for hold times between 30 min and 8 h at 1525°C. The limited grain growth is attributed primarily to the large fraction of porosity. Micrographs of 603 ppm SiO₂ singly doped and 529 ppm Na₂O and 603 ppm SiO₂ co-doped samples heated for 8 h after heating for 8 h at 1525°C are compared in Figure 3.7. Both samples are only 92-94% dense and thus it was difficult to prepare polished micrographs without some grain pull-out.

3.4 Discussion

To understand the above effects, we first note from the Al₂O₃-Na₂O phase diagram [5] that Na₂O is insoluble in α -Al₂O₃. A few platelet shaped grains with high aspect ratios were observed in the microstructures of sintered Na₂O-doped samples (Figure 3.8). Due to their morphology and literature reports, [6–10] it is assumed that these grains are a type of β -Al₂O₃. Four types of β -Al₂O₃ exist; two of them, β -Al₂O₃ (Na₂O·11Al₂O₃) and β'' -Al₂O₃ (Na₂O·5Al₂O₃), form in the binary system Na₂O-Al₂O₃ [11,12]. The determination of which type of β -Al₂O₃ forms and the conditions of formation were not the subject of this work, so these analyses were not performed.

Sodium aluminate (NaAlO₂) is reported to form at temperatures as low as 900°C, [13] and β'' -Al₂O₃ (Na₂O·5Al₂O₃) can be synthesized at temperatures as low as 1100 °C [6,14,15]. Therefore, we hypothesize that either sodium aluminate or β'' -Al₂O₃ forms before the onset of densification and that the presence of the

second phases on the surface of the Al_2O_3 particles retards the initial shrinkage of Na_2O -doped samples at $\sim 1050^\circ\text{C}$. However, we did not observe any $\beta\text{-Al}_2\text{O}_3$ type grains in the samples at this temperature. Alternatively, as discussed below, Na_2O may interact with the 103 ppm of intrinsic SiO_2 in the sample.

We hypothesize that the initial grain boundaries in the as-received Al_2O_3 are wetted with the intrinsic impurities such as Na_2O , CaO , TiO_2 and SiO_2 . Doping with Na_2O and SiO_2 changes the relative grain boundary chemistries and the properties of the respective grain boundary liquids. In the presence of a grain boundary liquid, densification occurs by a solution-precipitation sintering process, and thus, the rate of densification is controlled by either interface reaction between the grain boundary liquid and Al_2O_3 grains, or by the diffusion of Al^{3+} through the liquid grain boundary film. Al^{3+} diffusion is rate-limiting at 1525°C since it has been shown for molten glass systems that Al^{3+} has lower ionic diffusion rates than O^{2-} [16]. For diffusion-controlled densification, the densification rate is given by [17, 18]

$$\frac{d\left(\frac{\Delta\rho}{\rho}\right)}{dt} = \frac{A\delta D_l C_0 \gamma_{lv} \Omega}{kT} r_s^{-4} \quad (3.1)$$

and for interface reaction-controlled densification, the densification rate is given by

$$\frac{d\left(\frac{\Delta\rho}{\rho}\right)}{dt} = \frac{BK C_0 \gamma_{lv} \Omega}{kT} r_s^{-2} \quad (3.2)$$

where A and B are geometric factors, δ is the thickness of the liquid film, D_l is the diffusion coefficient of Al^{3+} in the liquid, C_0 is the equilibrium solute concentration, K the interface reaction constant, γ_{lv} is the liquid surface tension, Ω is the molecular volume of the solid, r_s is the particle radius, k is the Boltzmann constant and T is absolute temperature.

Equations 3.1 and 3.2 can be used to gain insights into the rate-limiting densification mechanisms during liquid phase sintering by evaluating their ratio [17, 18]

$$\alpha = \frac{A\delta D_l}{BK} r_s^{-2} \quad (3.3)$$

In general, for $\alpha > 1$, densification is controlled by the interface reaction, since D_l is relatively high. For $\alpha < 1$, densification is controlled by diffusion, and for $\alpha = 1$ both mechanisms contribute equally to densification [18]. Since the product

of the grain boundary thickness and the diffusion coefficient greatly influences the rate-determining mechanism, δD_l and the interface reaction constant K were examined in more detail.

Because the main impurities in Bayer aluminas are SiO_2 and Na_2O , the Al_2O_3 - SiO_2 - Na_2O ternary phase diagram [5] was utilized to evaluate the effects of dopant type and concentration on solubility of Al_2O_3 in the grain boundary liquid. It is assumed that the system approaches thermodynamic equilibrium upon holding at 1525°C , and thus the equilibrium composition of the liquid at 1525°C can be calculated from the ternary phase diagram (Figure 3.9). For simplification, we considered only Al_2O_3 , SiO_2 and Na_2O for the analysis, and assumed that all impurities/dopants are located in the grain boundaries. It was stated earlier that Na_2O is not soluble in Al_2O_3 , and it has been reported in the literature that SiO_2 segregates at the grain boundaries in Al_2O_3 [19]. Figure 3.9 shows the liquidus projection of the Al_2O_3 - SiO_2 - Na_2O ternary phase diagram. The red solid lines connecting the Al_2O_3 end member to the Na_2O - SiO_2 side are binary cuts through the ternary (isoplethal sections) and correspond to some of the $\text{Na}_2\text{O}/\text{SiO}_2$ ratios investigated in this study. The red dashed line is the isotherm at 1525°C for the part of the phase diagram where α - Al_2O_3 and liquid are in equilibrium. The blue dash-dot line and the green dotted line are eutectic lines along which β - Al_2O_3 or mullite is stable with α - Al_2O_3 and a liquid. The isotherm and the eutectic lines are important for determining the stable phases and the composition of the liquid in the samples. If a binary cut intersects the isotherm (red dashed line) only α - Al_2O_3 and liquid are stable phases at 1525°C and the intersection point determines the composition of the liquid. If a binary cut intersects one of the two marked eutectic lines (blue dash-dot or green dotted) a third phase (β - Al_2O_3 or mullite) is stable in those samples, and the composition of the liquid at 1525°C is determined by the intersection point of the respective intersected eutectic line with the isotherm at 1525°C .

The Al_2O_3 - SiO_2 - Na_2O phase diagram demonstrates that a small amount of liquid is stable at 1525°C for all compositions investigated. Note that these overall compositions are all very close to the Al_2O_3 end member ($\sim 99.8\%$ Al_2O_3) and Na_2O and SiO_2 are insoluble in Al_2O_3 . Isoplethal sections (red solid lines in Figure 3.9) can be used to determine the stability and equilibrium composition of a liquid since the volume fractions of Na_2O and SiO_2 are known. Lambotte and

Chartrand [5] calculated isoplethal sections of the ternary phase diagram, and based on their calculations, the solubility of Al_2O_3 in the liquid at 1525°C in the samples was estimated based on the respective $\text{Na}_2\text{O}:\text{SiO}_2$ ratios (assuming a constant liquid density of 2.45 g/cm^3 [3, 20]). Likewise, the volume fractions of liquid and solid phases can be estimated since the doping and impurity concentrations of SiO_2 and Na_2O are known. Table 3.2 summarizes the stable phases, the liquid compositions, and the total amount of liquid in the as-received and doped samples. Stable liquids at 1525°C are predicted for liquid compositions with $\text{Na}_2\text{O}:\text{SiO}_2$ ratios between 0.25 and 0.5. As described above, for higher Na_2O concentrations in the samples (global $\text{Na}_2\text{O}:\text{SiO}_2$ ratio > 0.5), $\alpha\text{-Al}_2\text{O}_3$, $\beta\text{-Al}_2\text{O}_3$ and a liquid with a $\text{Na}_2\text{O}:\text{SiO}_2$ ratio of 0.5 are stable. For sample compositions with higher SiO_2 concentrations (global $\text{Na}_2\text{O}:\text{SiO}_2$ ratio < 0.25) $\alpha\text{-Al}_2\text{O}_3$, mullite and a liquid with a $\text{Na}_2\text{O}:\text{SiO}_2$ ratio of 0.25 are stable. Since the global $\text{Na}_2\text{O}:\text{SiO}_2$ ratio in most of the samples investigated in this work is either > 0.5 or < 0.25 , the liquid in those samples had compositions of 0.5 or 0.25, respectively. As the $\text{Na}_2\text{O}:\text{SiO}_2$ ratio in the liquid increases from 0.25 to 0.5 the solubility of Al_2O_3 in the liquid increases from 18.4 vol.% to 21.6 vol.% [5]. The increased Al_2O_3 solubility leads to higher densification rates and higher densities in $\text{Na}_2\text{O}/\text{SiO}_2$ co-doped samples compared to singly SiO_2 -doped samples, regardless of the rate-limiting process.

Assuming fully dense samples and the liquid volume fractions reported in Table 3.2, we calculated the grain boundary thickness δ using:

$$\delta = 2 \frac{V_g \phi}{S_g (1 - \phi)} \quad (3.4)$$

where ϕ is the liquid volume fraction and V_g and S_g are the volume and the surface area based on the average grain size, respectively. For as-received and singly Na_2O -doped samples the grain boundary thickness is $< 0.3 \text{ nm}$ for all observed grain sizes. For $\text{Na}_2\text{O}/\text{SiO}_2$ -co-doped samples (603 ppm SiO_2) the grain boundary thickness is between 0.8 and 1.8 nm for grain sizes of $1 \text{ }\mu\text{m}$ and $2.5 \text{ }\mu\text{m}$, respectively. The calculated grain boundary thickness of singly SiO_2 -doped samples is similar to that of as-received samples, since mullite is predicted to form in the $\text{Al}_2\text{O}_3\text{-SiO}_2\text{-Na}_2\text{O}$ system for low Na_2O concentrations at 1525°C . However, mullite may not form in Bayer process Al_2O_3 due to the presence of other impurities, such as CaO , which, similar to Na_2O , lowers the eutectic temperature and acts as a network modifier

in the glass. Therefore, the grain boundary thicknesses of singly SiO₂-doped and Na₂O/SiO₂ co-doped samples are expected to be similar at ~ 1.8 nm. The amount of liquid in the samples and, therefore, the grain boundary thickness, is governed mainly by the amount of glass forming species in the samples, i.e. SiO₂.

The diffusion coefficient of Al³⁺ through the liquid grain boundary phase can be calculated with the Eyring relation

$$D_l = \frac{kT}{\eta\lambda} \quad (3.5)$$

where η is the viscosity of the grain boundary liquid and λ is the jump distance of the diffusion species, taken as the ionic diameter of an Al³⁺ (1.07 Å). Using viscosity data (range of 20 - 400 Pa*s) from the literature [21], we estimated the diffusion coefficients to be $\sim 1 \cdot 10^{-7}$ and $\sim 5 \cdot 10^{-9}$ cm²/s for Na₂O/SiO₂ co-doped and singly SiO₂-doped samples, respectively.

Although we can calculate values for grain boundary thickness (δ) and viscosity (η), an exact α -ratio cannot be determined using Equation 3.3 because we do not know the interface reaction constant (K). Nevertheless, assuming a reasonable K value from the literature ($K = 5 \cdot 10^{-8}$ m/s) [18] and assuming that the A/B ratio (A and B being geometrical factors) is on the order of 1, we estimated α to be $\sim 10^{-2}$ and ~ 1 for singly SiO₂-doped samples (603 ppm SiO₂) and Na₂O/SiO₂ co-doped samples (529/603 ppm), respectively. Thus, we conclude that at 1525°C densification of Bayer aluminas with low Na₂O/SiO₂ concentration ratios is governed by diffusion, whereas densification of Bayer aluminas with high Na₂O/SiO₂ concentration ratios can be governed by either diffusion or interface reaction.

The enhanced densification of Na₂O/SiO₂ co-doped samples compared to singly SiO₂-doped is attributed to two factors; the increased solubility of Al₂O₃ in the liquid grain boundary phase, and the enhanced diffusion of Al³⁺ ($\sim 5 \cdot 10^{-9}$ to $\sim 1 \cdot 10^{-7}$ cm²/s) through the liquid grain boundary. This effect of enhanced densification of Na₂O/SiO₂ co-doped samples compared to singly SiO₂-doped samples is observed in both the dilatometry curves and the densification kinetics data shown in Figure 3.2 and Figure 3.6, respectively.

It should be noted that a particular challenge for thermal processing studies with soda-based ceramics is Na₂O volatilization at relatively lower temperature than the sintering temperature. Soda by itself is highly volatile at temperatures

$< 1000^{\circ}\text{C}$ and the evaporation of soda from Na_2O containing technical ceramics such as sodium niobates [22] and $\beta\text{-Al}_2\text{O}_3$ during sintering is often reported. For example, $\beta\text{-Al}_2\text{O}_3$ ($\text{Na}_2\text{O}\cdot 11\text{Al}_2\text{O}_3$) has an appreciable Na_2O vapor pressure at temperatures $> 1400^{\circ}\text{C}$ [14], and when heated in air to $> 1500^{\circ}\text{C}$, $\beta\text{-Al}_2\text{O}_3$ converts to $\alpha\text{-Al}_2\text{O}_3$ by volatilization of Na_2O [14, 23]. Therefore, Na_2O evaporation from the samples during heating should be considered as samples might have somewhat lower Na_2O concentrations than assumed for the above calculations. Thus, for samples with low $\text{Na}_2\text{O}:\text{SiO}_2$ ratios, the liquid grain boundary phase may contain somewhat less Na_2O and the grain boundary thickness may be somewhat less than calculated. However, for singly Na_2O -doped samples and for co-doped samples with high $\text{Na}_2\text{O}:\text{SiO}_2$ ratios (e.g. $\text{Na}_2\text{O} \geq 529$ ppm for samples with 603 ppm SiO_2) the composition of the grain boundary liquid and the grain boundary thickness is not expected to change very much if Na_2O volatilizes. Consequently, even with Na_2O volatilization, the proposed sintering mechanisms do not change. The evaporation of Na_2O from Bayer Al_2O_3 samples will be further discussed in future work.

3.5 Summary

High concentrations of Na_2O in Bayer process Al_2O_3 powders inhibit densification in the initial sintering stage and retard densification up to the final sintering stage compared to powders with low Na_2O concentrations. However, Na_2O shows no adverse effect on the final density after longer hold times (≥ 3 h at 1525°C). The addition of SiO_2 to Bayer process Al_2O_3 powders substantially retards densification, starting at $\sim 1250^{\circ}\text{C}$, and samples containing as much as 603 ppm SiO_2 are 4% less dense than samples containing 103 ppm SiO_2 , even after hold times as long as 8 h at 1525°C . Co-doping with Na_2O and SiO_2 increases densification by 1 - 2.5% relative density relative to singly SiO_2 -doped samples. The observed differences in sintering behavior can be explained by a liquid phase sintering model. Diffusion and solubility of Al_2O_3 in the SiO_2 -based liquid in the grain boundaries is low at the temperatures used in this study, which explains the substantial retardation of densification by SiO_2 . As predicted from the phase diagram Na_2O increases the solubility of Al_2O_3 in the siliceous grain boundary phase. As predicted from viscosity data Na_2O enhances diffusion of Al^{3+} through the liquid grain boundary phase. Both factors contribute to the enhanced densification rates of samples with

high $\text{Na}_2\text{O}/\text{SiO}_2$ ratios compared to samples with low $\text{Na}_2\text{O}/\text{SiO}_2$ ratios.

Table 3.1. Physical and chemical characteristics of the as-received Bayer Al_2O_3 powder used in this study.

BET (m^2/g)	7.4
D_{50} (μm)	0.4
D_{90} (μm)	1.5
	ICP (ppm)
Al_2O_3	99.96 %
SiO_2	103
Na_2O (total)	29
Fe_2O_3	90
CaO	62
TiO_2	22
MgO	2

Table 3.2. Calculated compositions and amounts of liquid in as-received, singly doped and co-doped samples at 1525°C ($\alpha = \alpha\text{-Al}_2\text{O}_3$, $\beta = \beta\text{-Al}_2\text{O}_3$, L = liquid, M = mullite).

Global dopant concentration		Global Na ₂ O:SiO ₂ ratio	Na ₂ O:SiO ₂ ratio in Liquid	Composition of liquid (mol %)			Amount of liquid (vol. %)	Stable phases
ppm (wt.) Na ₂ O/SiO ₂	ppm (mol) Na ₂ O/SiO ₂			Na ₂ O	SiO ₂	Al ₂ O ₃		
As-received 29/103	48/175	0.27	0.25	17.9	63.4	19.7	0.03%	α +L
154/103- 1029/103	253/175- 1693/175	1.45-9.67	0.5	26.1	52.3	21.6	0.03%	α +L+ β
29/603	48/1023	0.05	0.25	16.3	65.3	18.4	0.03%	α +L+M
154/603	253/1023	0.25	0.25	16.3	65.3	18.4	0.16%	α +L
279/603	459/1023	0.45	0.45	24.5	54.6	20.8	0.19%	α +L
529/603	870/1023	0.85	0.5	26.1	52.3	21.6	0.22%	α +L+ β
1029/603	1693/1023	1.65	0.5	26.1	52.3	21.6	0.22%	α +L+ β

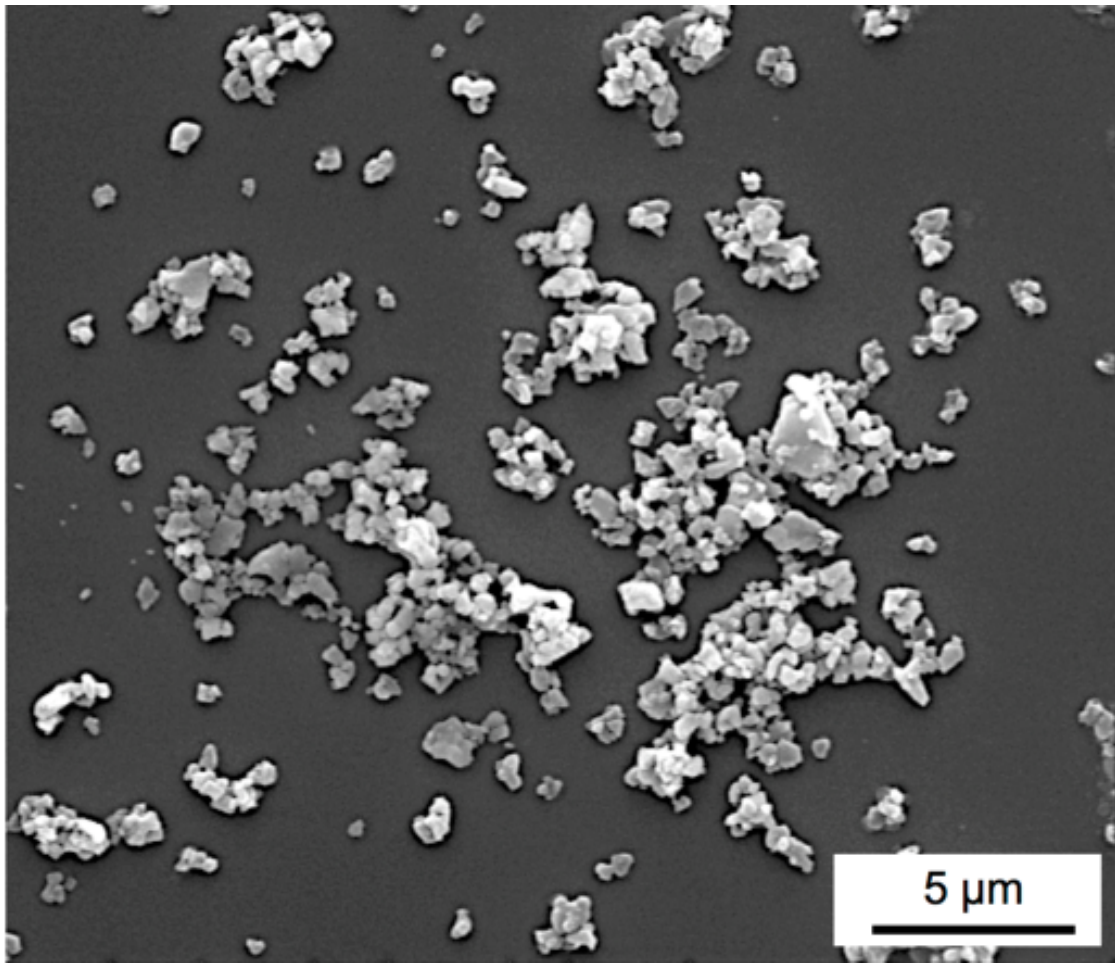


Figure 3.1. SEM image of as-received chemically purified Bayer Al₂O₃ powder used in this study.

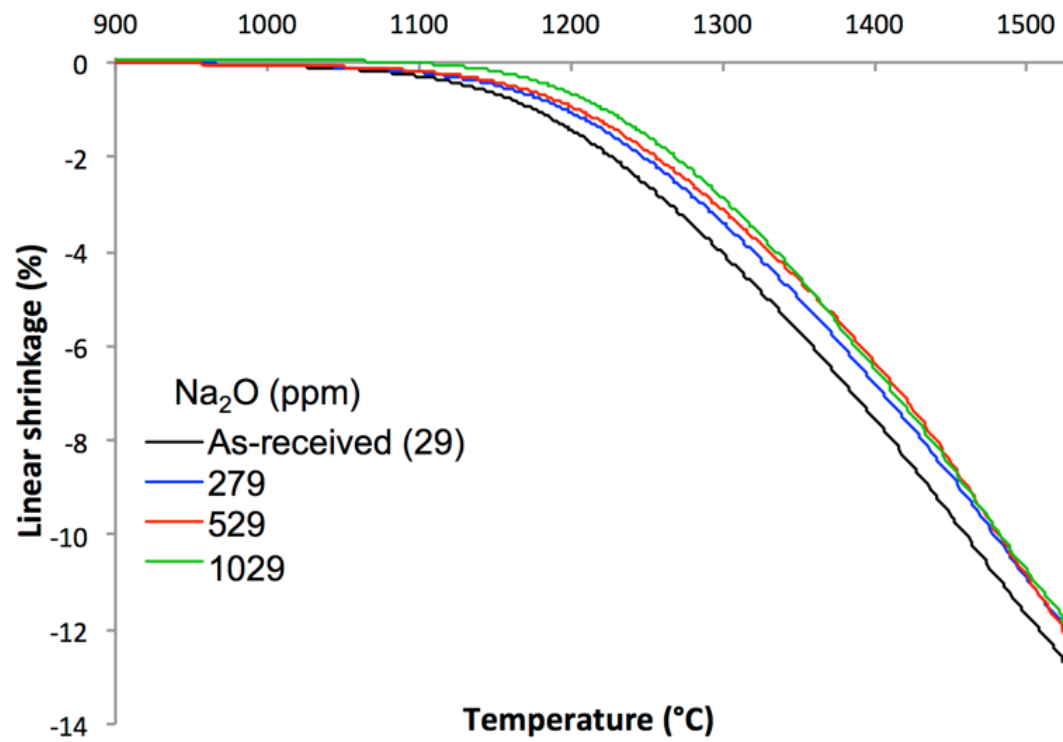


Figure 3.2. Dilatometer curves of as-received and singly Na₂O-doped samples heated at 10°C/min to 1525°C.

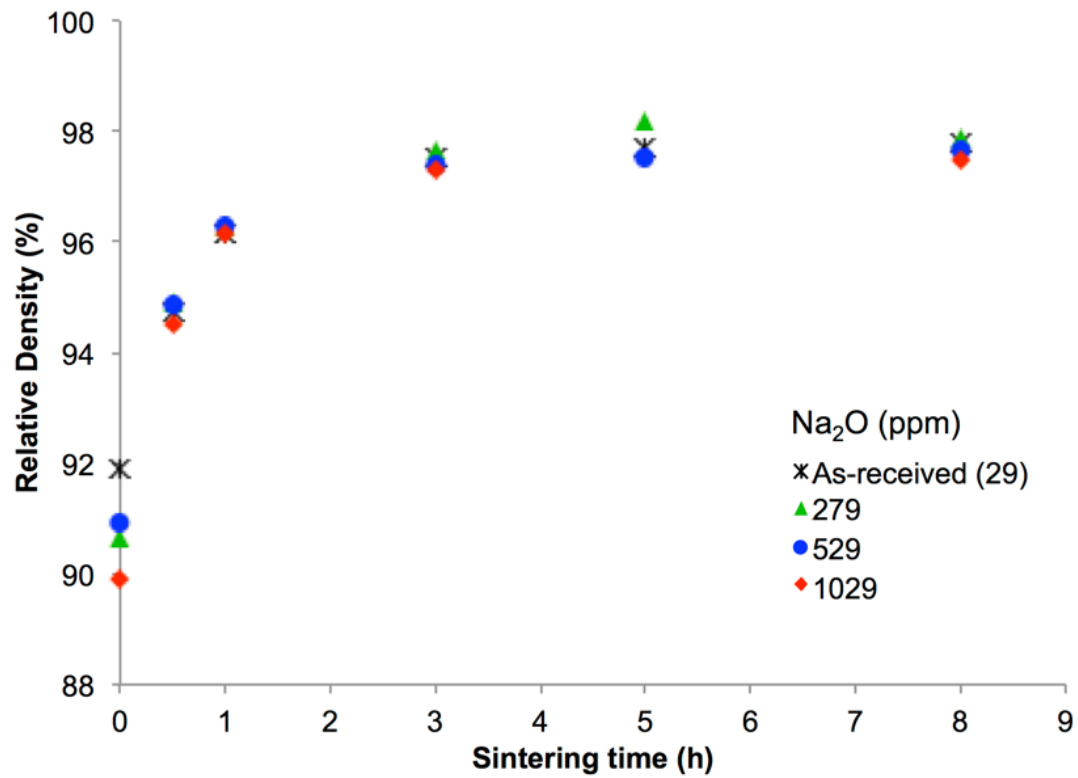


Figure 3.3. Densification kinetics of Bayer Al_2O_3 doped with different Na_2O concentrations and sintered at 1525°C .

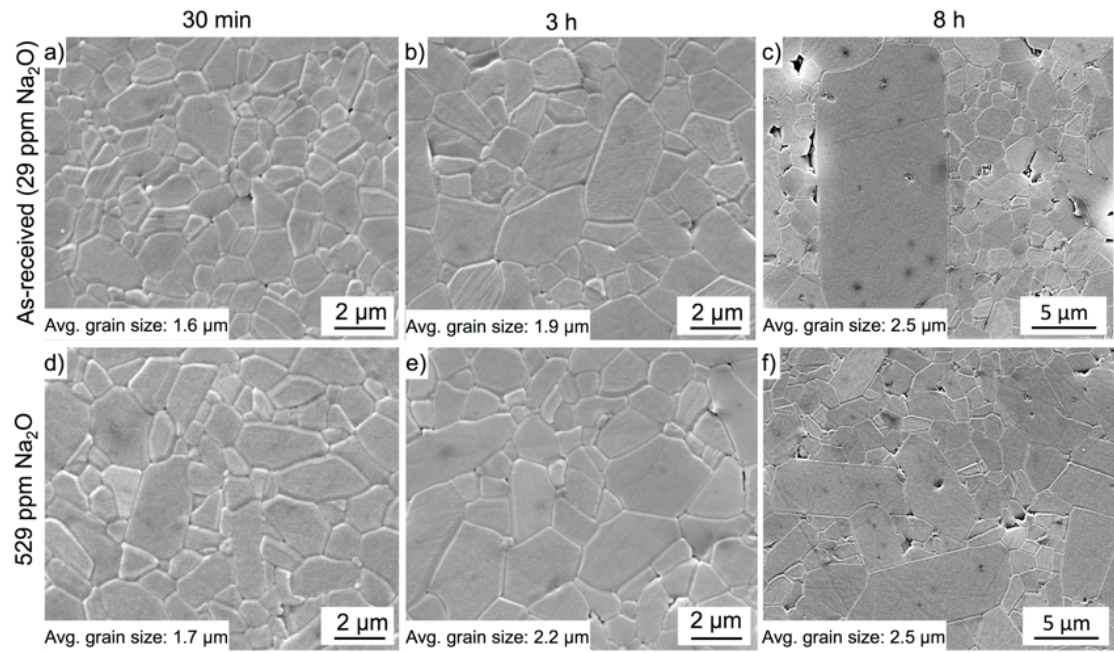


Figure 3.4. Microstructures of as-received and singly 529 ppm Na_2O doped samples after 30 min, 3 h and 8 h at 1525°C .

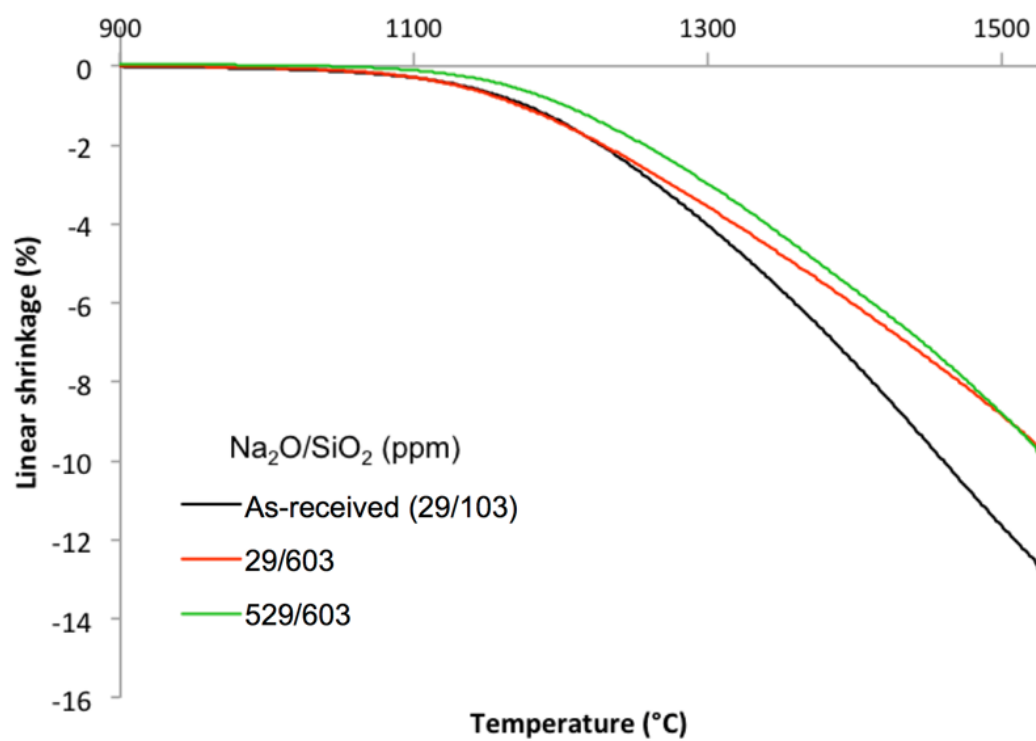


Figure 3.5. Dilatometer curves of as-received, singly SiO₂-doped, and Na₂O/SiO₂-doped Bayer Al₂O₃ heated at 10°C/min to 1525°C.

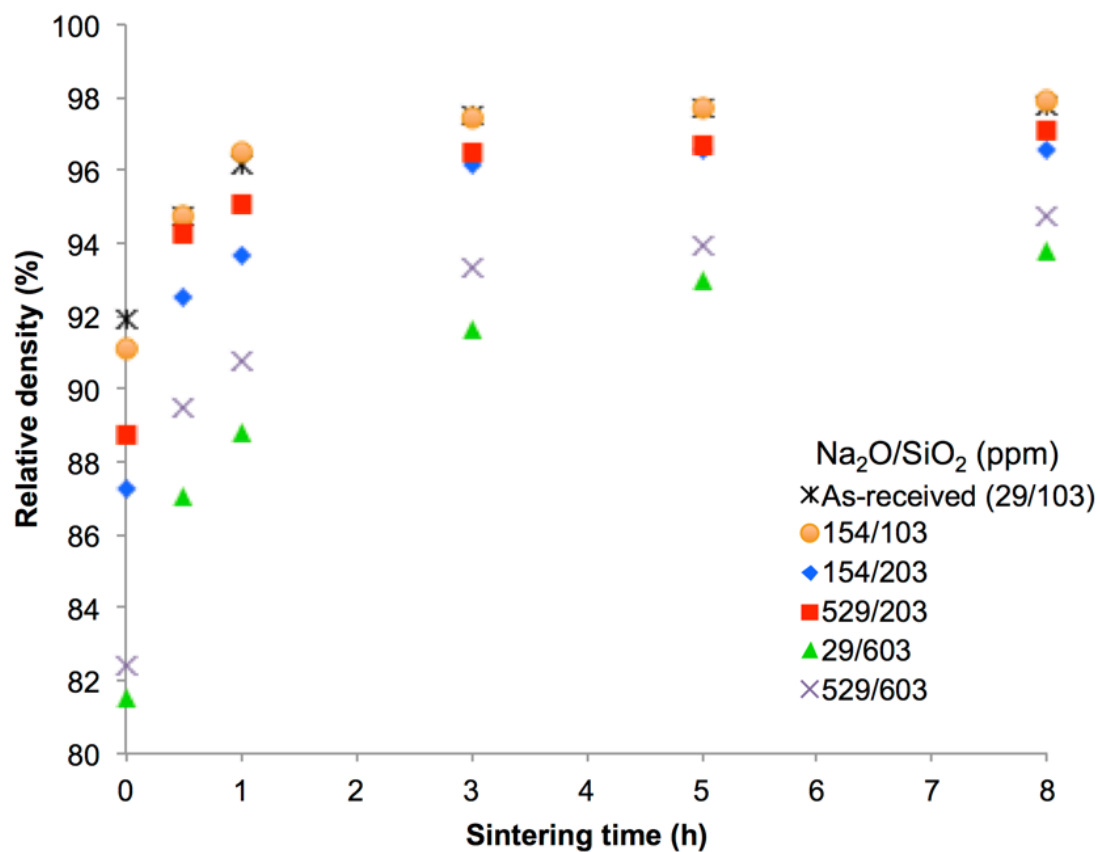


Figure 3.6. Densification kinetics of Bayer Al_2O_3 doped with different concentrations of Na_2O and SiO_2 at 1525°C .

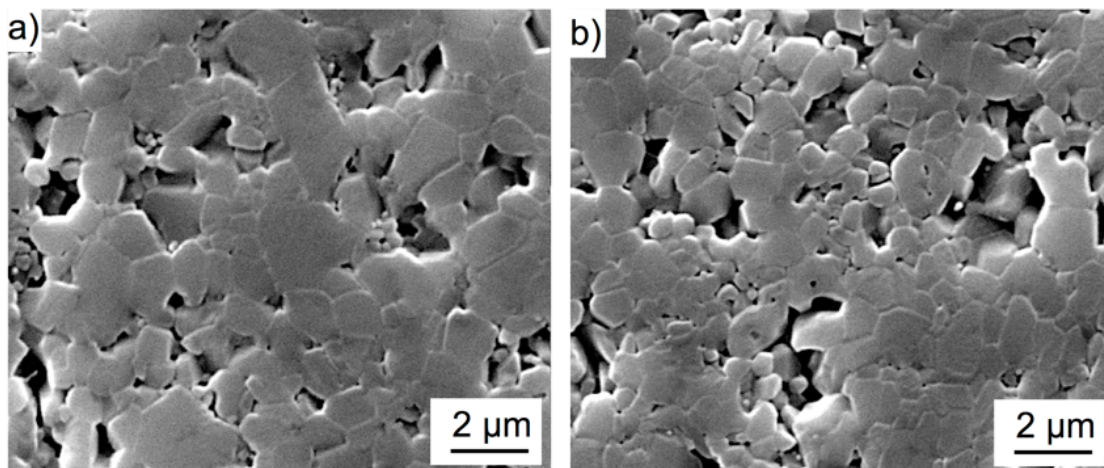


Figure 3.7. Microstructures of Bayer Al₂O₃ doped with a) 603 ppm SiO₂ and b) 529 ppm Na₂O and 603 ppm SiO₂ after heating at 1525°C for 8h.

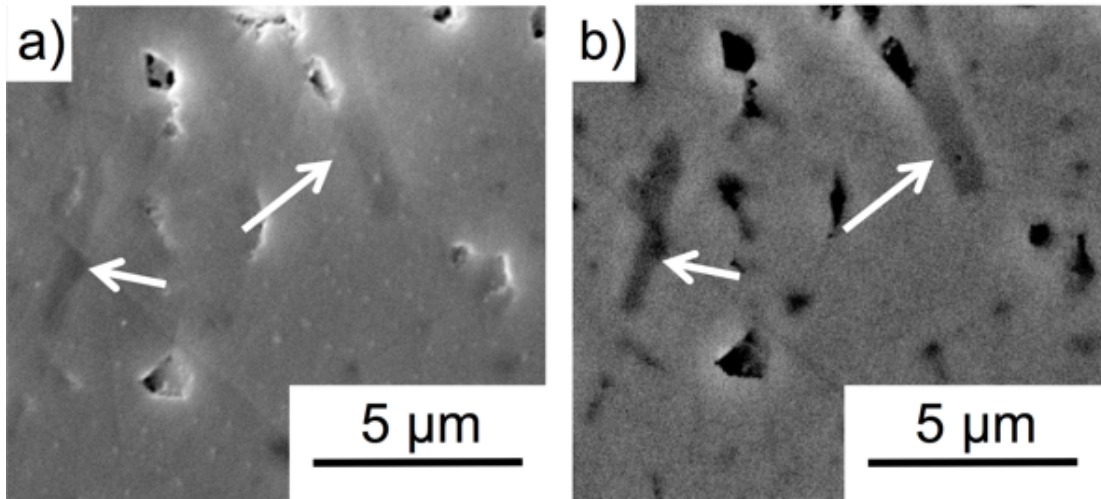


Figure 3.8. Micrographs of a sample doped with 1029 ppm Na_2O after sintering at 1525°C for 3 h. The micrographs were recorded using a) a secondary electron detector and b) a backscattered electron detector. The arrows point at the platelet shaped beta alumina grains that form in samples doped with Na_2O . The samples were not thermally etched.

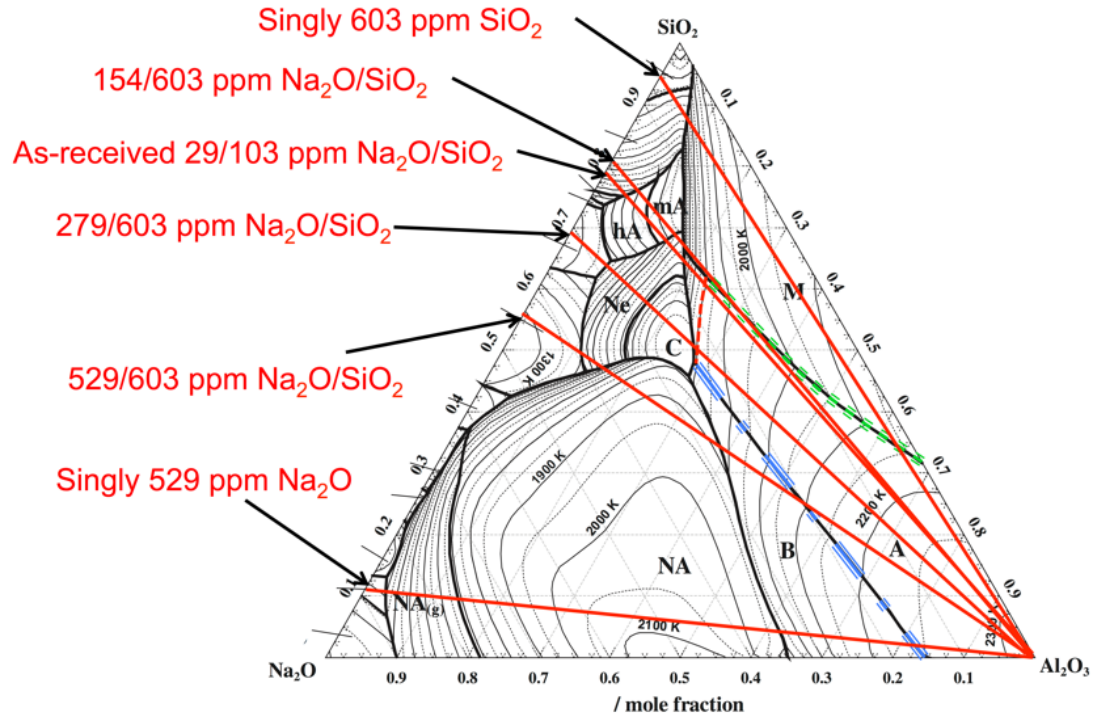


Figure 3.9. Liquidus projection of the Al_2O_3 - SiO_2 - Na_2O ternary phase diagram. The red solid lines are isoplethal cuts representing the samples investigated in this study. The red dashed line is the 1525°C isotherm where α - Al_2O_3 and liquid are in equilibrium. The blue dash-dot line and green dotted line are eutectic lines at which α - Al_2O_3 and liquid is in equilibrium with β - Al_2O_3 or mullite, respectively.

Chapter 4 | Powder Chemistry Effects on the Sintering Behavior of MgO-doped Bayer Alumina

4.1 Introduction

When in the Course of human events, it becomes necessary for one people to dissolve the political bands which have connected them with another, and to assume among the powers of the earth, the separate and equal station to which the Laws of Nature and of Nature's God entitle them, a decent respect to the opinions of mankind requires that they should declare the causes which impel them to the separation.

4.2 More Declaration

We hold these truths to be self-evident, that all men are created equal, that they are endowed by their Creator with certain unalienable Rights, that among these are Life, Liberty and the pursuit of Happiness. –That to secure these rights, Governments are instituted among Men, deriving their just powers from the consent of the governed, –That whenever any Form of Government becomes destructive of these ends, it is the Right of the People to alter or to abolish it, and to institute new Government, laying its foundation on such principles and organizing its powers in such form, as to them shall seem most likely to effect their Safety and Happiness. Prudence, indeed, will dictate that Governments long established should not be

changed for light and transient causes; and accordingly all experience hath shewn, that mankind are more disposed to suffer, while evils are sufferable, than to right themselves by abolishing the forms to which they are accustomed.

4.2.1 Some nonsense here

But when a long train of abuses and usurpations, pursuing invariably the same Object evinces a design to reduce them under absolute Despotism, it is their right, it is their duty, to throw off such Government, and to provide new Guards for their future security. –Such has been the patient sufferance of these Colonies; and such is now the necessity which constrains them to alter their former Systems of Government.

4.2.2 Some additional nonsense here

The history of the present King of Great Britain [George III] is a history of repeated injuries and usurpations, all having in direct object the establishment of an absolute Tyranny over these States. To prove this, let Facts be submitted to a candid world.

Chapter 5 | Powder Chemistry Effects on Grain Boundaries During Den-sification of Bayer Alumina

5.1 Introduction

When in the Course of human events, it becomes necessary for one people to dissolve the political bands which have connected them with another, and to assume among the powers of the earth, the separate and equal station to which the Laws of Nature and of Nature's God entitle them, a decent respect to the opinions of mankind requires that they should declare the causes which impel them to the separation.

5.2 More Declaration

We hold these truths to be self-evident, that all men are created equal, that they are endowed by their Creator with certain unalienable Rights, that among these are Life, Liberty and the pursuit of Happiness. –That to secure these rights, Governments are instituted among Men, deriving their just powers from the consent of the governed, –That whenever any Form of Government becomes destructive of these ends, it is the Right of the People to alter or to abolish it, and to institute new Government, laying its foundation on such principles and organizing its powers in such form, as to them shall seem most likely to effect their Safety and Happiness. Prudence, indeed, will dictate that Governments long established should not be

changed for light and transient causes; and accordingly all experience hath shewn, that mankind are more disposed to suffer, while evils are sufferable, than to right themselves by abolishing the forms to which they are accustomed. But when a long train of abuses and usurpations, pursuing invariably the same Object evinces a design to reduce them under absolute Despotism, it is their right, it is their duty, to throw off such Government, and to provide new Guards for their future security. —Such has been the patient sufferance of these Colonies; and such is now the necessity which constrains them to alter their former Systems of Government. The history of the present King of Great Britain [George III] is a history of repeated injuries and usurpations, all having in direct object the establishment of an absolute Tyranny over these States. To prove this, let Facts be submitted to a candid world.

Chapter 6 |

β -Al₂O₃: A Model System for the Formation of Second Phases in Al₂O₃

6.1 Introduction

When in the Course of human events, it becomes necessary for one people to dissolve the political bands which have connected them with another, and to assume among the powers of the earth, the separate and equal station to which the Laws of Nature and of Nature's God entitle them, a decent respect to the opinions of mankind requires that they should declare the causes which impel them to the separation.

6.2 More Declaration

We hold these truths to be self-evident, that all men are created equal, that they are endowed by their Creator with certain unalienable Rights, that among these are Life, Liberty and the pursuit of Happiness. –That to secure these rights, Governments are instituted among Men, deriving their just powers from the consent of the governed, –That whenever any Form of Government becomes destructive of these ends, it is the Right of the People to alter or to abolish it, and to institute new Government, laying its foundation on such principles and organizing its powers in such form, as to them shall seem most likely to effect their Safety and Happiness. Prudence, indeed, will dictate that Governments long established should not be

changed for light and transient causes; and accordingly all experience hath shewn, that mankind are more disposed to suffer, while evils are sufferable, than to right themselves by abolishing the forms to which they are accustomed. But when a long train of abuses and usurpations, pursuing invariably the same Object evinces a design to reduce them under absolute Despotism, it is their right, it is their duty, to throw off such Government, and to provide new Guards for their future security. —Such has been the patient sufferance of these Colonies; and such is now the necessity which constrains them to alter their former Systems of Government. The history of the present King of Great Britain [George III] is a history of repeated injuries and usurpations, all having in direct object the establishment of an absolute Tyranny over these States. To prove this, let Facts be submitted to a candid world.

Chapter 7 |

Summary and Future Work

7.1 Introduction

When in the Course of human events, it becomes necessary for one people to dissolve the political bands which have connected them with another, and to assume among the powers of the earth, the separate and equal station to which the Laws of Nature and of Nature's God entitle them, a decent respect to the opinions of mankind requires that they should declare the causes which impel them to the separation.

7.2 More Declaration

We hold these truths to be self-evident, that all men are created equal, that they are endowed by their Creator with certain unalienable Rights, that among these are Life, Liberty and the pursuit of Happiness. —That to secure these rights, Governments are instituted among Men, deriving their just powers from the consent of the governed, —That whenever any Form of Government becomes destructive of these ends, it is the Right of the People to alter or to abolish it, and to institute new Government, laying its foundation on such principles and organizing its powers in such form, as to them shall seem most likely to effect their Safety and Happiness. Prudence, indeed, will dictate that Governments long established should not be changed for light and transient causes; and accordingly all experience hath shewn, that mankind are more disposed to suffer, while evils are sufferable, than to right themselves by abolishing the forms to which they are accustomed. But when a long train of abuses and usurpations, pursuing invariably the same Object evinces

a design to reduce them under absolute Despotism, it is their right, it is their duty, to throw off such Government, and to provide new Guards for their future security. —Such has been the patient sufferance of these Colonies; and such is now the necessity which constrains them to alter their former Systems of Government. The history of the present King of Great Britain [George III] is a history of repeated injuries and usurpations, all having in direct object the establishment of an absolute Tyranny over these States. To prove this, let Facts be submitted to a candid world.

Bibliography

- [1] LOUET, N., M. GONON, and G. FANTOZZI (2005) "Influence of the amount of Na_2O and SiO_2 on the sintering behavior and on the microstructural evolution of a Bayer alumina powder," *Ceramics international*, **31**(7), pp. 981–987.
- [2] STANDARD, A. (2015) "B962-15 Standard Test Method for Density of Compacted or Sintered Powder Metallurgy (PM) Products Using Archimedes' Principle," .
URL www.astm.org
- [3] ——— (2013) "E112-13: Standard Test Methods for Determining Average Grain Size," *West Conshocken*.
URL www.astm.org
- [4] JUDD, M., B. PLUNKETT, and M. POPE (1974) "The thermal decomposition of calcium, sodium, silver and copper (II) acetates," *Journal of Thermal Analysis and Calorimetry*, **6**(5), pp. 555–563.
- [5] LAMBOTTE, G. and P. CHARTRAND (2013) "Thermodynamic modeling of the $(\text{Al}_2\text{O}_3 + \text{Na}_2\text{O})$, $(\text{Al}_2\text{O}_3 + \text{Na}_2\text{O} + \text{SiO}_2)$, and $(\text{Al}_2\text{O}_3 + \text{Na}_2\text{O} + \text{AlF}_3 + \text{NaF})$ systems," *The Journal of Chemical Thermodynamics*, **57**, pp. 306–334.
- [6] BROWNMILLER, L. T. and R. H. BOGUE (1932) "The system $\text{CaO}-\text{Na}_2\text{O}-\text{Al}_2\text{O}_3$," *American Journal of Science*, (138), pp. 501–524.
- [7] PABLOÁÑGALAN, L. and W. R. FOSTER (1959) "Investigation of Role of Beta Alumina in the System $\text{Na}_2\text{O}-\text{Al}_2\text{O}_3-\text{SiO}_2$," *Journal of the American Ceramic Society*, **42**(10), pp. 491–498.
- [8] RANKIN, G. A. and H. E. MERWIN (1916) "THE TERNARY SYSTEM $\text{CaO}-\text{Al}_2\text{O}_3-\text{MgO}$," *Journal of the American Chemical Society*, **38**(3), pp. 568–588.

- [9] RIDGWAY, R. R., A. A. KLEIN, and W. J. O'LEARY (1936) "The Preparation and Properties of So-called β -Alumina," *Transactions of the Electrochemical Society*, **70**(1), pp. 71–88.
- [10] DUNCAN, J. H. and W. E. C. CREYKE (1969) "FORMATION AND STABILITY OF BETA-AL₂O₃ IN ALPHA-AL₂O₃ CERAMICS," *TRANSACTIONS OF THE BRITISH CERAMIC SOCIETY*, **68**(3), p. 137.
- [11] SUTORIK, A. C., S. S. NEO, D. R. TREADWELL, and R. M. LAINE (1998) "Synthesis of Ultrafine β -Alumina Powders via Flame Spray Pyrolysis of Polymeric Precursors," *Journal of the American Ceramic Society*, **81**(6), pp. 1477–1486.
- [12] STEVENS, R. and J. G. P. BINNER (1984) "Structure, properties and production of β -alumina," *Journal of materials science*, **19**(3), pp. 695–715.
- [13] CHRISTIE, J. R., A. J. DARNELL, and D. F. DUSTIN (1978) "Reaction of molten sodium carbonate with aluminum oxide," *J. Phys. Chem.:(United States)*, **82**(1).
- [14] KUMMER, J. T. (1972) " β -alumina electrolytes," *Progress in solid state chemistry*, **7**, pp. 141–175.
- [15] VRIES, R. C. and W. L. ROTH (1969) "Critical Evaluation of the Literature Data on Beta Alumina and Related Phases: I, Phase Equilibria and Characterization of Beta Alumina Phases," *Journal of the American Ceramic Society*, **52**(7), pp. 364–369.
- [16] TERAJ, R. and R. HAYAMI (1975) "Ionic diffusion in glasses," *Journal of Non-Crystalline Solids*, **18**(2), pp. 217–264.
- [17] KWON, O. and G. L. MESSING (1990) "Kinetic Analysis of Solution-Precipitation During Liquid-Phase Sintering of Alumina," *Journal of the American Ceramic Society*, **73**(2), pp. 275–281.
- [18] KWON, O.-H. and G. L. MESSING (1991) "A theoretical analysis of solution-precipitation controlled densification during liquid phase sintering," *Acta metallurgica et materialia*, **39**(9), pp. 2059–2068.
- [19] PARK, C. W. and D. Y. YOON (2000) "Effects of SiO₂, CaO₂, and MgO additions on the grain growth of alumina," *Journal of the American ceramic society*, **83**(10), pp. 2605–2609.
- [20] DAY, D. E. and G. E. RINDONE (1962) "Properties of soda aluminosilicate glasses: I, refractive index, density, molar refractivity, and infrared absorption spectra," *Journal of the American Ceramic Society*, **45**(10), pp. 489–496.

- [21] WU, G., E. YAZHENSKIY, K. HACK, and M. MÜLLER (2015) “Viscosity model for oxide melts relevant to fuel slags. Part 2: The system $\text{SiO}_2\text{--Al}_2\text{O}_3\text{--CaO--MgO--Na}_2\text{O--K}_2\text{O}$,” *Fuel Processing Technology*, **138**, pp. 520–533.
- [22] POPOVIC, A., L. BENCZE, J. KORUZA, B. MALIC, and M. KOSEC (2012) “Knudsen effusion mass spectrometric approach to the thermodynamics of $\text{Na}_2\text{O--Nb}_2\text{O}_5$ system,” *International Journal of Mass Spectrometry*, **309**, pp. 70–78.
- [23] GALLUP, J. (1935) “The transformation of aluminum oxide from the beta to the alpha form,” *Journal of the American Ceramic Society*, **18**(1–12), pp. 144–148.

Vita

Tobias Frueh

The details of my childhood are inconsequential.